The enzyme Rnf completes the pathway for forming propionate during fermentation in *Prevotella*

Running title: Rnf and propionate formation

Bo Zhang, Christopher Lingga, Hannah De Groot, Timothy J. Hackmann#

Department of Animal Science, University of California, Davis, CA, USA

#Address correspondence to Timothy J. Hackmann, tjhackmann@ucdavis.edu

ABSTRACT

Propionate is a microbial metabolite that is formed in the gastrointestinal tract, and it affects host physiology as a source of energy and signaling molecule. Despite the importance of propionate, the biochemical pathways responsible for its formation are not clear in all microbes. For the succinate pathway used during fermentation, a key enzyme appears to be missing—one that can oxidize ferredoxin and reduce NAD. Here we show that Rnf [ferredoxin--NAD(+) oxidoreductase (Na(+)-transporting)] is this key enzyme in two abundant bacteria of the rumen (*Prevotella brevis* and *Prevotella ruminicola*). We found these bacteria form propionate, succinate, and acetate with the classic succinate pathway. At first, this pathway appears unbalanced, forming reduced ferredoxin and oxidized NAD in excess. If this continued unabated, fermentation would halt within 1.5 s. We found these bacteria solve this problem by oxidizing ferredoxin and reducing NAD with Rnf. This is demonstrated using growth experiments, genomics, proteomics, and enzyme assays. Genomic and phenotypic data suggest many bacteria use Rnf similarly. We cataloged fermentation products of >1,400 species of prokaryotes, and nearly 10% formed propionate, succinate, and acetate. Over 40% of species carrying out this fermentation also had genes for Rnf. This work shows Rnf is important to propionate formation in many bacteria from the environment, and it provides fundamental knowledge for manipulating fermentative propionate production.

INTRODUCTION

Metabolites formed via anaerobic fermentation in the gastrointestinal of mammals have great effects on the host physiology and health (1, 2). The major metabolites formed by gut bacteria during fermentation of dietary carbohydrates are short-chain fatty acids (SCFAs). As one of the major SCFAs, propionate can affect satiety and glucose homeostasis in humans (3, 4). It has beneficial effects on beta-cell function to maintain healthy glucose homeostasis (5). Recently, it has been demonstrated that propionate can suppress colorectal cancer growth (6, 7), while excess levels of propionate may lead to Alzheimer's disease by inducing hyperammonemia (8). Furthermore, propionate also plays important roles in other animals, such as ruminants. It is a major source of glucose for the ruminants, and about 50% of glucose is from propionate (9). Propionate formation in the rumen of ruminants is negatively related with methane emission, since they compete for metabolic hydrogen in the rumen. Favoring propionate formation could mitigate methane emissions (10). Realizing its importance in human health, agricultural production, and the environment, studies focusing on biochemical pathways have revealed many enzymes responsible for fermentative propionate production (11, 12).

Three biochemical pathways are responsible for fermentative propionate production from dietary carbohydrates, including the succinate pathway, the acrylate pathway, and the propanediol pathway (11, 12). Propionate is most commonly formed using the succinate pathway and in combination with acetate. This pathway involves the conversion of succinate to propionate via methylmalonyl-CoA. Some organisms with this pathway include *Bacteroides fragilis* (13) and *Selenomonas ruminantium* (14). The acrylate pathway involves the conversion of lactate to lactoyl-CoA, acryloyl-CoA, propionyl-CoA and propionate, e.g. *Coprococcus catus* (11) and

Megasphaera elsdenii (15). Some gut commensal bacteria, such as *Roseburia inulinivorans* (16), carry out the propanediol pathway to from propionate from deoxy sugars.

Despite decades of study, one major biochemical pathway (i.e. the succinate pathway) for forming propionate has unknown steps. When glucose is the substrate, this pathway has a problem: it forms excess amounts of reduced ferredoxin (Fd_{red}), a redox cofactor (Fig. 1A) (17). This cofactor is formed by the enzyme pyruvate:ferredoxin oxidoreductase (EC 1.2.7.1), and no step is known to oxidize it back to ferredoxin (Fd_{ox}) during this pathway. Similarly, the pathway forms oxidized NAD (NAD_{ox}), with no step to reduce it back to reduced NAD (NAD_{red}). This is an apparent problem in both prokaryotes (17, 18) and eukaryotes (19). These unknown steps are important because if Fd_{ox} and NAD_{red} is exhausted (not regenerated), fermentation will halt.

We hypothesized that the enzyme Rnf fills in the missing steps (Fig. 1B). The enzyme Rnf [ferredoxin--NAD(+) oxidoreductase (Na(+)-transporting), EC 7.2.1.2] simultaneously oxidizes Fd_{red} and reduces NAD_{ox}, solving two problems at once. This enzyme plays a similar role in other pathways, such as one metabolizing caffeate (20). Recently, we found Rnf genes in many propionate-forming bacteria from the rumen (17). Here we study two of these rumen bacteria in detail and find that they indeed use Rnf in forming propionate (or its precursor, succinate). We show this using growth experiments, genomics, proteomics, and enzyme assays. Further, we find Rnf is common in bacteria that form propionate (or succinate), with 44 type strains from many habitats encoding it. This work suggests Rnf is important to propionate formation in many bacteria from the environment.

RESULTS

Prevotella form propionate, succinate, and acetate during fermentation

Our hypothesis was that fermentation of glucose to propionate, succinate, and acetate uses Rnf. We studied this in two bacteria from the rumen (*Prevotella brevis* GA33 and *Prevotella ruminicola* 23). The first step was to verify that these organisms form propionate, succinate, and acetate and in the ratios expected (Fig. 1). We grew these bacteria on media containing glucose and ammonia, then analyzed the culture for several products. For *P. brevis* GA33, we used a medium that also contained yeast extract and trypticase, as it would not grow on media with glucose only.

Both species formed large amounts of succinate and acetate (Fig. 2A). Propionate was formed in large amounts by *P. ruminicola* 23, whereas it was formed in only trace amounts by *P. brevis* GA33 (Fig. S1). The ratio of succinate and propionate to acetate was approximately 2:1. They also formed formate, D-lactate, and L-lactate, but only in trace amounts. These results follow our expectations (Fig. 1).

Neither species formed H_2 (Fig. S2). As a control, we analyzed gas samples from *S. ruminantium* HD4, a propionate-forming bacterium that forms H_2 in trace amounts (21). We were indeed able to detect H_2 formation by this organism (Fig. S2). This result shows that if *Prevotella* formed H_2, even in trace amounts, we would have been able to detect it.

To check how accurately we measured products, we calculated carbon and hydrogen recovery (Fig. 2B and C). A recovery of 100% indicates that all carbon (or hydrogen) at the start of incubation was recovered in products measured at the end. We found recoveries were near or above 100%. For *P. brevis* GA33, values were above 100% because our calculations did not account for trypticase and yeast extract also in the medium of this bacterium. The high recoveries of carbon and hydrogen indicate that we measured all products accurately.

In sum, our work shows that *Prevotella* form propionate, succinate, and acetate as the sole products of fermentation (Fig. 2D). Additionally, they form these products in the ratio expected (Fig. 1).

Fermentation in *Prevotella* appears to be unbalanced

We hypothesized that *Prevotella* use Rnf to balance fermentation. Without this enzyme, fermentation should produce excess NAD_{ox} and Fd_{red}. We determined if this was indeed the case for *Prevotella*.

We calculated the quantity of NAD_{ox} and Fd_{red} produced during the experiments above (Table S1). Our calculations revealed that excess NAD_{ox} and Fd_{red} were indeed formed. The amount was 2.7 NAD_{ox} and 2.3 Fd_{red} per 3 glucose (Table S1). This was even higher than expected (Fig. 1) and owed to additional NAD_{ox} and Fd_{red} being formed during production of cells (particularly lipid) (Table S2). This calculation did not include the activity of Rnf, and it shows without this enzyme, fermentation would indeed be unbalanced.

Next, we calculated how long cells could sustain such an unbalanced fermentation. We calculated that all Fd_{ox} would be consumed and fermentation would halt within 1.5 s. This calculation assumes 2.3 Fd_{red} per 3 glucose fermented (Table S1), 667 nmol glucose fermented (g dry cells)$^{-1}$ s^{-1} (see Materials and Methods), 75 nmol total ferredoxin/g wet cells (22), wet cells are 10% dry mass, and all ferredoxin starts as Fd_{ox}. Without Rnf, cells could sustain fermentation only for seconds (or less).

We performed calculations on *P. ruminicola* 23 only. To calculate the quantity of NAD_{ox} and Fd_{red} formed during production of cells, we assumed macromolecules were synthesized from

glucose and ammonia (Table S2). This would have been a bad assumption for *P. brevis* GA33, where macromolecules could have come from trypticase and yeast extract.

Our calculation points to an apparent excess of NAD_{ox} and Fd_{red} formed during fermentation and growth. It shows a critical need for Rnf or a similar enzyme.

Prevotella have Rnf [ferredoxin--NAD(+) oxidoreductase (Na(+)-transporting)]

Having established a need for an enzyme like Rnf, we determined if this activity of Rnf is indeed possessed by *Prevotella*. Genomics, proteomics, and enzyme assays were used to test its presence.

We found Rnf in both the genome and proteome (Fig. 3, Table S3, Table S4). The genomes of both species had genes for all six subunits of this enzyme (Fig. 3A). Proteomics revealed genes for four subunits were expressed in *P. brevis* GA33 and three in *P. ruminicola* 23 (Fig. 3B). Our methods were exhaustive and used multiple sample types (cell extract, cell membrane) and acquisition methods (data-dependent acquisition, data-independent acquisition). The two subunits we never detected (RnfA and RnfE) are predicted to be integral proteins, which are challenging targets in proteomics. These subunits have evaded detection even in purified Rnf (23).

After finding evidence of Rnf in the genome and proteome, we tested for its catalytic activity [ferredoxin--NAD(+) oxidoreductase] with enzyme assays (Fig. 3C). To do so, we measured formation of NAD_{red} by cell membranes after adding Fd_{red}. Using these assays, we found that cell membrane of both *Prevotella* species had activity (Fig. 3C). The activity depended on adding both Fd_{red} and NAD_{ox}. Further, activity was localized to the membrane; activity in cytoplasmic contents was low for *P. brevis* GA33 (3.1 [0.5] (mean [standard error of mean]) mU/mg) and undetectable for *P. ruminicola* 23. These experiments show *Prevotella* had activity

of Rnf, and the properties were as expected. Likewise, these experiments rule out the presence of a similar enzyme in the cytoplasm [a cytoplasmic ferredoxin--NAD(+) oxidoreductase].

At first, activity observed in the cell membrane appeared low. However, we found higher activity after correcting for activity of NADH dehydrogenase that leads to consumption of NAD_{red} formed in the assay (Fig. 3C). This correction is commonly done for other NADH-dependent enzymes [see, for example, Asanuma and Hino (24)], and it makes sense to do it with Rnf. We found still higher activity after performing a partial purification of Rnf (by solubilizing cell membranes in detergent) (Fig. 3C). This shows that activity, at first low, is indeed present and on par with other membrane-bound enzymes (see below).

To verify that this activity was due to Rnf, not another enzyme, we determined its dependence on sodium ion (Fig. 4). In most species, Rnf pumps sodium ions (to create a gradient) and thus depends on them for high activity (23, 25, 26). We found that *P. brevis* GA33 did not grow without sodium, showing a general dependence on this ion (Fig. 4A). We found the same for *P. ruminicola* 23 (data not shown). Further, when we directly tested if sodium ion stimulated the catalytic activity of Rnf, we found that it did (Fig. 4B).

Our enzyme assays required Fd_{red}, which we generated using a system similar to Schoelmerich et al. (27). Specifically, we purified ferredoxin from *C. pasteurianum* 5, then we reduced it with pyruvate and crude pyruvate:ferredoxin oxidoreductase. The crude pyruvate:ferredoxin oxidoreductase was cytoplasmic contents from the organism in which Rnf was tested (*P. brevis* GA33 or *P. ruminicola* 23). We verified that the crude pyruvate:ferredoxin oxidoreductase worked as intended. First, we used it to detect activity of Rnf in *Pseudobutyrivibrio ruminis* A12-1. We found activity of 50.0 [1.9] mU/mg, which is similar to the value found by schoelmerich et al. (27) for the same organism. Second, we screened it for

158 activity of interfering enzymes, including a cytoplasmic ferredoxin--NAD(+) oxidoreductase and
159 pyruvate dehydrogenase. We found these interfering activities were low or undetectable (see
160 results above for cytoplasmic ferredoxin--NAD(+) oxidoreductase and see below for pyruvate
161 dehydrogenase). These results show this system is appropriate for generating Fd_{red} in Rnf assays.

162 In sum, our work at the genomic proteomic, and enzymatic level establishes that *Prevotella*
163 have Rnf. With it, *Prevotella* can handle excess NAD_{ox} and Fd_{red} produced during fermentation.

164 **_Prevotella_ have other enzymes needed to form fermentation products**

165 After finding that Rnf was present in *Prevotella*, we determined if other enzymes forming
166 propionate, succinate, and acetate were also present. This was important to confirm that redox
167 cofactors (NAD_{ox} and Fd_{red}) are produced in the pathway as expected. Again, we relied on
168 genomics, proteomics, and enzyme assays.

169 We found enzymes of the classic succinate pathway in the genome and proteome (Fig. 5,
170 Table S3, Table S4). When using proteomics, we found cytoplasmic enzymes were well detected
171 (Fig. 5A). Membrane-bound proteins were also detected, though some subunits (corresponding to
172 integral proteins) were missed (as with Rnf) (Fig. 5B). The membrane-bound proteins Nqr (EC
173 7.2.1.1) and fumarate reductase (EC 1.3.5.1) in our bacteria have also been detected in *Prevotella*
174 *bryantii* $B_1$4 (28), where they have been characterized. Together, these enzymes form a pathway
175 where Rnf is needed to regenerate NAD_{red} and Fd_{ox}.

176 There was one enzyme missing in *P. brevis* GA33 and another in *P. ruminicola* 23 (Fig.
177 5A). In *P. brevis* GA33, an enzyme of glycolysis (enolase) was missing in the genome and
178 proteome. This has no easy explanation but has been found previously in the genome (17, 29). In
179 *P. ruminicola* 23, an enzyme for converting succinate to propionate was likewise missing. Despite

this finding, there is evidence the enzyme is present (or substituted by a similar enzyme). The conversion of succinate to propionate is well known to require vitamin B_{12} (30), and *P. ruminicola* 23 formed propionate only when this vitamin was in the media (data not shown). Others have found the same for this bacterium (31). With a few possible exceptions, our work shows that *Prevotella* have the expected enzymes in the genome and proteome.

After finding evidence in the genome and proteome, we tested for catalytic activity of key enzymes (Table 2). We focused mostly on enzymes that generate redox cofactors used by Rnf. We detected activity in all cases expected. For example, we found activity of malate dehydrogenase (EC 1.1.1.37), which produces NAD_{ox} (used by Rnf). A similar enzyme producing $NADP_{ox}$ (EC 1.1.1.82) was also detected, but with lower activity. Our work confirms that *Prevotella* have the expected enzymes for forming propionate, succinate, and acetate—including those that form NAD_{ox} and Fd_{red}. Rnf is needed to complete this pathway.

Rnf is important in many organisms forming propionate, succinate, and acetate

We wanted to see if Rnf is distributed widely in organisms that form propionate, succinate, and acetate. To do so, we used genomic and phenotypic data for prokaryotes from *Bergey's Manual of Systematics of Archaea and Bacteria* (Table S5).

We first determined how many prokaryotes form propionate, succinate, and acetate during fermentation. We constructed a heat map to summarize fermentation products reported for organisms in *Bergey's Manual* (Fig. 6). This encompasses 39 products from over 1,400 type strains (Table S5). We found that prokaryotes that form exclusively propionate/succinate and acetate (no other products) represent about 10% of the total. Thus, fermentations that form propionate, succinate, and acetate are common.

202 Next, we determined the occurrence of Rnf genes in prokaryotes (Fig. 7, Table S6). We
203 used a total of n = 3,775 type strains for which a genome sequence was available. We found that
204 Rnf genes were uncommon in prokaryotes in general (Fig. 7A). However, these genes were more
205 common in prokaryotes that are fermentative and even more so in those that form propionate,
206 succinate, and acetate. This shows a clear importance of Rnf in such organisms.

207 In total, 44 type strains encoded Rnf and formed propionate, succinate, and acetate during
208 fermentation. A phylogenetic tree shows that these strains are diverse, and they belong to 15
209 genera (Fig. 7B). Examining their habitats shows that they come from the gut, aquatic sediment,
210 anaerobic digesters, and elsewhere (Fig. 7C, Table S7). Together, these results suggest Rnf is
211 important to propionate formation not just in *Prevotella*, but to many organisms from various
212 habitats.

213 **Organisms have alternatives to Rnf, but they are uncommon**

214 By oxidizing Fd_{red} and reducing NAD_{ox}, Rnf is one enzyme that fills in the missing step of the
215 pathway we study. However, other alternatives can be imagined. To see if any alternatives were
216 common, we used the same genomic and phenotypic data for prokaryotes as before.

217 We considered five possible pathways (Fig. S3, Table S6, Table S7). One pathway
218 involves the enzyme pyruvate dehydrogenase (EC 1.2.4.1) (Fig. S3A). When this enzyme replaces
219 pyruvate:ferredoxin oxidoreductase, the resulting pathway is balanced without Rnf. This in fact is
220 the pathway originally proposed for propionate formation 60 years ago (32). However, it is
221 uncommon; only 17% of organisms that form propionate, succinate, and acetate encode this
222 enzyme. The four other pathways—involving prototypical hydrogenase (EC 1.12.7.2), bifurcating

hydrogenase (EC 1.12.1.4), formate dehydrogenase (EC 1.17.5.3), or *Campylobacter*-type Nuo (33, 34)—are even less common (Fig. S3).

None of these five pathways was found in *Prevotella*. Their genomes did not encode the appropriate enzymes (Tables S3, S4, and S6). We tested cell extracts for catalytic activity of pyruvate dehydrogenase, and we did not find any in *P. brevis* GA33 or *P. ruminicola* 23. We found similar results for cytoplasmic contents and that there was no detectable activity of pyruvate dehydrogenase. As a control, we tested cell extracts of a bacterium with pyruvate dehydrogenase [*E. coli* BL21(DE3)pLysS], and we found high activity (>1 U/mg protein). We also found high activity when spiking cell extract of this bacterium into cell extracts of *P. brevis* GA33 and *P. ruminicola* 23. These controls show our assay worked. Further, we found *P. brevis* GA33 and *P. ruminicola* 23 formed only trace quantities of formate, and they formed no H_2 (Fig. 2, Fig. S2). In sum, there are no obvious alternatives to Rnf to *Prevotella*. This underscores the importance of Rnf in organisms forming propionate, succinate, and acetate.

DISCUSSION

Our study shows Rnf is important to forming propionate during fermentation. In *Prevotella*, we show that fermentation is apparently unbalanced and produces excess Fd_{red} and NAD_{ox}. Rnf handles the excess Fd_{red} and NAD_{ox} by converting them back to Fd_{ox} and NAD_{red}. No other enzyme (or combination of enzymes) had this activity. Rnf thus completes the pathway and allows fermentation to continue.

The pathway for forming propionate has been studied for over 60 years (32), yet the need for an enzyme like Rnf was only recently recognized (17, 18). A likely reason Rnf has been overlooked is the pathway was first elucidated in propionibacteria (32). Propionibacteria have

pyruvate dehydrogenase, which, if used, would make the pathway balanced without Rnf (Fig. S3) (32). A pathway with pyruvate dehydrogenase, though plausible, appears seldom used. First, our work shows few organisms forming propionate also encode pyruvate dehydrogenase. Second, propionibacteria themselves may not use this enzyme. Recent work shows they also have pyruvate:ferredoxin oxidoreductase, which is expressed (18, 35) and required for normal growth (18). In *Prevotella*, we found activity of pyruvate:ferredoxin oxidoreductase, but not pyruvate dehydrogenase. Thus, there is a real need for an enzyme like Rnf.

Given this need, we looked for direct evidence of Rnf in *Prevotella*, and we used multiple approaches. Growth experiments showed that fermentation would be unbalanced without Rnf. They showed the problem was serious, and without Rnf, fermentation would halt within 1.5 s. Genomics and proteomics showed that *Prevotella* both encoded and expressed Rnf. Enzyme assays showed *Prevotella* had catalytic activity of Rnf, and its properties were as expected. Our experiments also ruled out alternatives to Rnf. For example, our enzyme assays ruled out presence of a similar enzyme in the cytoplasm [a cytoplasmic ferredoxin--NAD(+) oxidoreductase]. Our growth experiments ruled out H_2 or formate as other ways of balancing fermentation. In sum, multiple lines of evidence show that *Prevotella* have Rnf and that it balances fermentation.

Our work shows Rnf is encoded by many organisms that form propionate, succinate, and acetate. This result suggests Rnf is important not just to *Prevotella* but many other organisms. Our results also show additional strategies must exist for balancing redox cofactors. We show five strategies, though none is as common as Rnf. Further, we do not examine eukaryotes, even though they have the same problem (19).

Propionate is most commonly formed by succinate pathway, but the acrylate pathway is an alternative. Rnf would be important to either pathway. Though the two pathways involve different

carbon intermediates, both produce excess NAD_{ox} and Fd_{red} (2 each per 3 glucose) [see (17)]. Indeed, Rnf is in the proteome of one bacterium that uses the acrylate pathway (36). During ethanol metabolism via the acrylate pathway in a propionate-producer *Anaerotignum neopropionicum*, Rnf is predicted to operate in the reverse direction to reduce Fd_{ox} and oxidize NAD_{red} at the expense of ATP (37). Furthermore, Rnf could be important for NADH regeneration in strains of *Clostridium saccharoperbutylacetonicum* metabolically engineered to produce propionate via the acrylate pathway (38). As an aside, one study suggested that *P. ruminicola* 23 uses the acrylate pathway, not the succinate pathway (39). Our study and others (31) do not support this idea, but Rnf would be important regardless.

The knowledge that Rnf is involved in propionate production is critical for manipulating fermentative propionate production. Modification of metabolic pathways involving redox reactions for synthesis of target metabolites often introduces redox imbalance, which affects the growth and production of the engineered microbes (40). Several cofactor-engineering strategies have been developed to solve the problematic redox imbalance issue (41, 42); however, it is difficult to address this when the knowledge about enzymes involved in redox balance are unknown.

In sum, Rnf completes the pathway for forming propionate formation during fermentation. It has importance in the bacteria we study in the rumen and for bacteria from many other habitats. This work is key to understanding how propionate is formed in the environment and to manipulating its production.

MATERIALS AND METHODS

Organisms

P. brevis GA33 and *P. ruminicola* 23 were obtained from the ATCC. *Clostridium pasteurianum* 5 and *Pseudobutyrivibrio ruminis* A12-1 were obtained from the DSMZ. *Selenomonas ruminantium* HD4 was obtained from Michael Flythe (USDA-ARS, Lexington, KY) and originally isolated by Marvin Bryant (43). *Escherichia coli* BL21(DE3)pLysS was from Promega.

Media and growth

Except where noted, strains were grown anaerobically under O_2-free CO_2 and with serum bottles with butyl rubber stoppers (44, 45). The inoculant (seed) was 0.1 mL volume of a stationary-phase culture. The temperature of growth was 37°C.

P. brevis GA33 and *S. ruminantium* HD4 were cultured on the medium PC+VFA (46). *P. ruminis* A12-1 was cultured on a complex medium as described by Schoelmerich et al. (27). *P. ruminicola* 23 was cultured on medium BZ. We developed this defined medium from a complex medium (47). Per liter, the medium contained 8 g glucose, 0.6 g K_2HPO_4, 0.45 g KH_2PO_4, 0.45 g $(NH_4)_2SO_4$, 0.9 g NaCl, 92 mg $MgSO_4$, 0.12 g $CaCl_2 \cdot 2H_2O$, 2 mL of 0.5 g/L hemin in 10 mM NaOH, 1 mL 0.1% (w/v) resazurin, 1 mL trace element SL-9 (48), 10 mL DSMZ-medium-141 Wolin's vitamin solution, 0.1 mg vitamin B_{12}, 322.7 µL isobutyric acid, 322.7 µL 2-methylbutyric acid, 322.7 µL valeric acid, 322.7 µL isovaleric acid, 4 g Na_2CO_3, and 1.2 g L-cysteine·HCl·H_2O. Glucose, Wolin's vitamin solution, and vitamin B_{12} were added to medium BZ after autoclaving. *C. pasteurianum* 5 was cultured on a glucose medium in 1-L Pyrex bottle sealed with stoppers. Per liter, the medium contained 20 g glucose, 15.329 g K_2HPO_4, 1.5 g KH_2PO_4, 0.1 g NaCl, 98 mg

309 $MgSO_4$, 10 mg $Na_2MoO_4 \cdot 2H_2O$, 1 g NH_4Cl, 50 mg $FeSO_4 \cdot 7\ H_2O$, 5 mg 4-aminobenzoic acid, and
310 1 mg biotin. *E. coli* BL21(DE3)pLysS was cultured aerobically on Luria-Bertani medium.

311 Growth of cultures was measured by removing 1-mL aliquots with a syringe and measuring
312 optical density at 600 nm (OD_{600}) in cuvettes in a Thermo Scientific Genesys 20
313 spectrophotometer. The sample was diluted with 0.9% (w/v) NaCl as needed to remain within the
314 linear range of the instrument.

315 **Analysis of fermentation products and cells**

316 Three, 70-mL cultures were inoculated and grown to the late-log phase (OD_{600} = 1.3 for *P. brevis*
317 GA33 and OD_{600} = 4.0 for *P. ruminicola* 23). Cells were harvested by centrifugation (21,100 × *g*
318 for 20 min at 4°C). The supernatant was stored at -20°C. Cell pellets were resuspended in ddH_2O
319 and harvested by centrifugation (21,100 × *g* for 30 min at 4°C). Pellets were transferred to
320 aluminum pans with ddH_2O and dried at 105 °C overnight. The dry mass of cells was determined
321 by weighing the pan with dried pellet (while still hot) (49). After cooling, an aliquot of pellet was
322 submitted for elemental analysis (C, H, N) by Intertek (Whitehouse, NJ). The cooled pellet was
323 reweighed to correct for any water absorbed.

324 Supernatant was analyzed for glucose and fermentation products according to Zhang et al.
325 (50) with modifications. Specifically, acetate was measured by gas chromatography rather than
326 enzymatic assay. Ethanol was measured with a commercial kit from Megazyme (product code K-
327 ETOH).

328 One aliquot of culture (5-mL) was also collected at the start of the incubation. Cells were
329 removed, and supernatant was analyzed as above. The inoculant for cultures was 0.1 mL of a late-
330 log phase culture. The dry mass of cells in this inoculant was determined by methods above. The

331 elemental composition (C, H, N) was assumed to be the same as cells inoculated and grown to the
332 late-log phase.

333 **Recovery of carbon and hydrogen**

334 We calculated recovery of carbon in cells and fermentation products. Recovery is defined as the
335 (total carbon at end)/(total carbon at start) × 100%.

336 Total carbon (mmol C L^{-1}) was the sum of carbon in cells, glucose, fermentation acids, and
337 CO_2. For CO_2, we defined the concentration at the start as 0. The concentration at the end was
338 calculated from stoichiometry, assuming -1 CO_2/formate, 1 CO_2/acetate, -1 CO_2/succinate, 2
339 CO_2/butyrate, 2 CO_2/isobutyrate, 1 CO_2/valerate, 1 CO_2/isovalerate, and 1 CO_2/ethanol [after
340 Hackmann et al. (51)]. CO_2 formed during cell synthesis was ignored.

341 Recovery of hydrogen was calculated analogously. For H_2O, we defined the concentration
342 at the start (mmol H L^{-1}) as 0. We calculated the concentration at the end (mmol H L^{-1}) from
343 stoichiometry, assuming 1 H_2O/acetate, 1 H_2O/propionate, and 1 H_2O/succinate [after Hackmann
344 et al. (51)]. H_2O formed during cell synthesis was ignored.

345 **Rate of glucose fermentation**

346 We measured rate of glucose fermentation by *P. ruminicola* 23 in the mid-exponential phase.
347 Samples of culture were collected at 4 points during this phase [where ln(OD_{600}) increased linearly
348 over time]. The glucose concentration (mmol L^{-1}) was measured as above. The dry cell weight (g
349 dry cell L^{-1}) was calculated from OD_{600} (referring to samples where both OD_{600} and weight were
350 known). The rate of glucose consumption [nmol glucose (g dry cell)$^{-1}$ s^{-1}] was directly calculated.
351 The rate of glucose fermentation was assumed to be glucose consumption × 0.642 (see Table S1).
352 The final value for three biological replicates was 667 nmol glucose fermented (g dry cell)$^{-1}$ s^{-1}.

Proteomics

We used proteomics to determine what genes were expressed in the cells of *P. brevis* GA33 and *P. ruminicola* 23. Peptide samples from cell extract and cell membrane were prepared and analyzed using LC-MS (see Text S1 for details).

Enzyme assays

We measured activities of enzymes in cell extract, cell membrane, and cytoplasmic contents. Assays were performed following Zhang et al (50). The temperature and other conditions were as reported in Table 1. One unit of activity is defined as 1 μmol of product formed per min. To correct Rnf activity for NADH dehydrogenase activity, we added to its value the activity measured for Nqr (see Table 2).

Samples (cell extract, cell membrane, cytoplasmic contents) were prepared according to Text S1. When required, ferredoxin was purified from *C. pasteurianum* 5 was according to reference (52) with modifications (see Text S1).

Other chemical analyses

Protein was measured using the Bradford method (53). The standard was bovine serum albumin. H_2 was measured with gas chromatography (see Text S1).

Information for organisms in Bergey's Manual

We collected phenotypic, genomic, and other information for organisms in *Bergey's Manual of Systematics of Archaea and Bacteria* (54). All n = 1,836 articles for genera in *Bergey's Manual* was downloaded. Names and written descriptions of n = 8,026 type strains were then extracted from the text. We used R scripts from Hackmann and Zhang (55) to automate this process. To

collect phenotypic information, we read written descriptions of the type strains. This information included fermentative ability and major fermentation endproducts. To collect genomic information, R scripts from Hackmann and Zhang (55) were used. The scripts first extracted out the organism's taxonomy and article link from the written description. The scripts then used the taxonomy to find an organism's GOLD organism ID, GOLD project ID, and IMG genome ID.

Searches for genes and proteins

We searched genomes for genes involved in forming propionate, succinate, and acetate. To do so, we used IMG/M database (56), the IMG/M genome ID for each genome, and the KEGG Orthology (KO) ID for each gene (57). For some genes, we searched for the COG (58) or pfam (59) ID instead. For hydrogenases, we followed methods in Text S1.

For each gene, we report the respective enzyme name, enzyme symbol, EC number, and biochemical reaction. This information came from KEGG (57) and HydDB (60). An enzyme was considered present in the genome if genes for all subunits was found. A reaction was considered present if at least one isozyme was found.

Other bioinformatic analyses

Proteomes were searched for proteins using locus tags for genes above. Phylogenetic trees were constructed according to Hackmann and Zhang (55). We identified habitats of organisms forming propionate, succinate, and acetate using *Bergey's Manual* (54), BacDive (61), and information from public culture collections. Structures of proteins were predicted using ColabFold (62), then they were visualized with PyMOL according to Hackmann (63).

Statistics

A one-sided *t*-tests was used to determine if mean yield of fermentation products and mean values of enzymatic activity was greater than 0. *P*-values reported are for that test.

Data availability

The LC-MS data have been deposited in the Proteomics Identification (PRIDE) Archive with the dataset identifier PXD034119.

ACKNOWLEDGMENTS

We thank Dr. Gabriela Grigorean of the UC Davis Proteomics Core for performing LC-MS analysis. This work was supported by an Agriculture and Food Research Initiative Competitive Grant [grant no. 2018-67015-27495] and Hatch Project [accession no. 1019985] from the United States Department of Agriculture National Institute of Food and Agriculture.

REFERENCES

1. Fan Y, Pedersen O. 2021. Gut microbiota in human metabolic health and disease. Nat Rev Microbiol 19:55-71.
2. Krautkramer KA, Fan J, Backhed F. 2021. Gut microbial metabolites as multi-kingdom intermediates. Nat Rev Microbiol 19:77-94.
3. Blaak EE, Canfora EE, Theis S, Frost G, Groen AK, Mithieux G, Nauta A, Scott K, Stahl B, van Harsselaar J, van Tol R, Vaughan EE, Verbeke K. 2020. Short chain fatty acids in human gut and metabolic health. Benef Microbes 11:411-455.
4. Hosseini E, Grootaert C, Verstraete W, Van de Wiele T. 2011. Propionate as a health-promoting microbial metabolite in the human gut. Nutr Rev 69:245-58.

5. Pingitore A, Chambers ES, Hill T, Maldonado IR, Liu B, Bewick G, Morrison DJ, Preston T, Wallis GA, Tedford C, Castanera Gonzalez R, Huang GC, Choudhary P, Frost G, Persaud SJ. 2017. The diet-derived short chain fatty acid propionate improves beta-cell function in humans and stimulates insulin secretion from human islets in vitro. Diabetes Obes Metab 19:257-265.

6. Ryu TY, Kim K, Son MY, Min JK, Kim J, Han TS, Kim DS, Cho HS. 2019. Downregulation of PRMT1, a histone arginine methyltransferase, by sodium propionate induces cell apoptosis in colon cancer. Oncol Rep 41:1691-1699.

7. Ryu TY, Kim K, Han TS, Lee MO, Lee J, Choi J, Jung KB, Jeong EJ, An DM, Jung CR, Lim JH, Jung J, Park K, Lee MS, Kim MY, Oh SJ, Hur K, Hamamoto R, Park DS, Kim DS, Son MY, Cho HS. 2022. Human gut-microbiome-derived propionate coordinates proteasomal degradation via HECTD2 upregulation to target EHMT2 in colorectal cancer. ISME J 16:1205-1221.

8. Killingsworth J, Sawmiller D, Shytle RD. 2021. Propionate and Alzheimer's Disease. Frontiers in Aging Neuroscience 12:580001.

9. Bergman EN. 1990. Energy contributions of volatile fatty acids from the gastrointestinal tract in various species. Physiol Rev 70:567-90.

10. Wang K, Xiong B, Zhao X. 2022. Could propionate formation be used to reduce enteric methane emission in ruminants? Sci Total Environ 855:158867.

11. Reichardt N, Duncan SH, Young P, Belenguer A, McWilliam Leitch C, Scott KP, Flint HJ, Louis P. 2014. Phylogenetic distribution of three pathways for propionate production within the human gut microbiota. ISME J 8:1323-35.

12. Louis P, Flint HJ. 2017. Formation of propionate and butyrate by the human colonic microbiota. Environ Microbiol 19:29-41.

13. Macy JM, Ljungdahl LG, Gottschalk G. 1978. Pathway of succinate and propionate formation in *Bacteroides fragilis*. J Bacteriol 134:84-91.

14. Paynter MJ, Elsden SR. 1970. Mechanism of propionate formation by *Selenomonas ruminantium*, a rumen micro-organism. J Gen Microbiol 61:1-7.

15. Hino T, Kuroda S. 1993. Presence of lactate dehydrogenase and lactate racemase in *Megasphaera elsdenii* grown on glucose or lactate. Appl Environ Microbiol 59:255-9.

16. Scott KP, Martin JC, Campbell G, Mayer CD, Flint HJ. 2006. Whole-genome transcription profiling reveals genes up-regulated by growth on fucose in the human gut bacterium "*Roseburia inulinivorans*". J Bacteriol 188:4340-9.

17. Hackmann TJ, Ngugi DK, Firkins JL, Tao J. 2017. Genomes of rumen bacteria encode atypical pathways for fermenting hexoses to short-chain fatty acids. Environ Microbiol 19:4670-4683.

18. McCubbin T, Gonzalez-Garcia RA, Palfreyman RW, Stowers C, Nielsen LK, Marcellin E. 2020. A pan-genome guided metabolic network reconstruction of five *Propionibacterium* species reveals extensive metabolic diversity. Genes (Basel) 11.

19. Müller M, Mentel M, van Hellemond JJ, Henze K, Woehle C, Gould SB, Yu RY, van der Giezen M, Tielens AG, Martin WF. 2012. Biochemistry and evolution of anaerobic energy metabolism in eukaryotes. Microbiol Mol Biol Rev 76:444-95.

20. Imkamp F, Biegel E, Jayamani E, Buckel W, Müller V. 2007. Dissection of the caffeate respiratory chain in the acetogen *Acetobacterium woodii*: identification of an Rnf-type NADH dehydrogenase as a potential coupling site. J Bacteriol 189:8145-53.

460 21. Scheifinger CC, Linehan B, Wolin MJ. 1975. H_2 production by *Selenomonas ruminantium*
461 in the absence and presence of methanogenic bacteria. Appl Microbiol 29:480-3.
462 22. Schonheit P, Brandis A, Thauer RK. 1979. Ferredoxin degradation in growing *Clostridium*
463 *pasteurianum* during periods of iron deprivation. Arch Microbiol 120:73-6.
464 23. Kuhns M, Trifunovic D, Huber H, Muller V. 2020. The Rnf complex is a Na^+ coupled
465 respiratory enzyme in a fermenting bacterium, *Thermotoga maritima*. Commun Biol 3:431.
466 24. Asanuma N, Hino T. 2000. Activity and properties of fumarate reductase in ruminal
467 bacteria. J Gen Appl Microbiol 46:119-125.
468 25. Biegel E, Müller V. 2010. Bacterial Na^+-translocating ferredoxin:NAD^+ oxidoreductase.
469 Proc Natl Acad Sci U S A 107:18138-42.
470 26. Hess V, Gallegos R, Jones JA, Barquera B, Malamy MH, Müller V. 2016. Occurrence of
471 ferredoxin:NAD^+ oxidoreductase activity and its ion specificity in several Gram-positive
472 and Gram-negative bacteria. PeerJ 4:e1515.
473 27. Schoelmerich MC, Katsyv A, Dönig J, Hackmann TJ, Müller V. 2020. Energy
474 conservation involving two respiratory circuits. Proc Natl Acad Sci 117:1167-1173.
475 28. Schleicher L, Trautmann A, Stegmann DP, Fritz G, Gatgens J, Bott M, Hein S, Simon J,
476 Seifert J, Steuber J. 2021. A sodium-translocating module linking succinate production to
477 formation of membrane potential in *Prevotella bryantii*. Appl Environ Microbiol
478 87:e0121121.
479 29. Seshadri R, Leahy SC, Attwood GT, Teh KH, Lambie SC, Cookson AL, Eloe-Fadrosh EA,
480 Pavlopoulos GA, Hadjithomas M, Varghese NJ, Paez-Espino D, Perry R, Henderson G,
481 Creevey CJ, Terrapon N, Lapebie P, Drula E, Lombard V, Rubin E, Kyrpides NC,
482 Henrissat B, Woyke T, Ivanova NN, Kelly WJ, collaborators Hp. 2018. Cultivation and

sequencing of rumen microbiome members from the Hungate1000 Collection. Nat Biotechnol 36:359-367.

30. Stadtman ER, Overath P, Eggerer H, Lynen F. 1960. The role of biotin and vitamin B_{12} coenzyme in propionate metabolism. Biochem Biophys Res Commun 2:1-7.

31. Strobel HJ. 1992. Vitamin B_{12}-dependent propionate production by the ruminal bacterium *Prevotella ruminicola* 23. Appl Environ Microbiol 58:2331-3.

32. Allen SH, Kellermeyer RW, Stjernholm RL, Wood HG. 1964. Purification and properties of enzymes involved in the propionic acid fermentation. J Bacteriol 87:171-87.

33. Weerakoon DR, Olson JW. 2008. The *Campylobacter jejuni* NADH:ubiquinone oxidoreductase (complex I) utilizes flavodoxin rather than NADH. J Bacteriol 190:915-25.

34. Franke T, Deppenmeier U. 2018. Physiology and central carbon metabolism of the gut bacterium *Prevotella copri*. Mol Microbiol 109:528-540.

35. Dank A, van Mastrigt O, Boeren S, Lillevang SK, Abee T, Smid EJ. 2021. *Propionibacterium freudenreichii* thrives in microaerobic conditions by complete oxidation of lactate to CO_2. Environ Microbiol 23:3116-3129.

36. Moreira JPC, Diender M, Arantes AL, Boeren S, Stams AJM, Alves MM, Alves JI, Sousa DZ. 2021. Propionate production from carbon monoxide by synthetic cocultures of *Acetobacterium wieringae* and propionigenic bacteria. Appl Environ Microbiol 87:e0283920.

37. Benito-Vaquerizo S, Parera Olm I, de Vroet T, Schaap PJ, Sousa DZ, Martins Dos Santos VAP, Suarez-Diez M. 2022. Genome-scale metabolic modelling enables deciphering ethanol metabolism via the acrylate pathway in the propionate-producer *Anaerotignum neopropionicum*. Microb Cell Fact 21:116.

506 38. Baur T, Wentzel A, Durre P. 2022. Production of propionate using metabolically
507 engineered strains of *Clostridium saccharoperbutylacetonicum*. Appl Microbiol
508 Biotechnol doi:10.1007/s00253-022-12210-8.
509 39. Wallnofer P, Baldwin RL. 1967. Pathway of propionate formation in *Bacteroides*
510 *ruminicola*. J Bacteriol 93:504-5.
511 40. Akhtar MK, Jones PR. 2014. Cofactor engineering for enhancing the flux of metabolic
512 pathways. Front Bioeng Biotechnol 2:30.
513 41. Liu J, Li H, Zhao G, Caiyin Q, Qiao J. 2018. Redox cofactor engineering in industrial
514 microorganisms: strategies, recent applications and future directions. J Ind Microbiol
515 Biotechnol 45:313-327.
516 42. Montano Lopez J, Duran L, Avalos JL. 2022. Physiological limitations and opportunities
517 in microbial metabolic engineering. Nat Rev Microbiol 20:35-48.
518 43. Bryant MP. 1956. The characteristics of strains of *Selenomonas* isolated from bovine
519 rumen contents. J Bacteriol 72:162-7.
520 44. Tao JY, Diaz RK, Teixeira CRV, Hackmann TJ. 2016. Transport of a fluorescent analogue
521 of glucose (2-NBDG) versus radiolabeled sugars by rumen bacteria and *Escherichia coli*.
522 Biochemistry 55:2578-2589.
523 45. Tao J, McCourt C, Sultana H, Nelson C, Driver J, Hackmann TJ. 2019. Use of a fluorescent
524 analog of glucose (2-NBDG) to identify uncultured rumen bacteria that take up glucose.
525 Appl Environ Microbiol 85:e03018-18.
526 46. Dai X, Hackmann TJ, Lobo RR, Faciola AP. 2020. Lipopolysaccharide stimulates the
527 growth of bacteria that contribute to ruminal acidosis. Appl Environ Microbiol 86.

528 47. Villas-Boas SG, Noel S, Lane GA, Attwood G, Cookson A. 2006. Extracellular
529 metabolomics: a metabolic footprinting approach to assess fiber degradation in complex
530 media. Anal Biochem 349:297-305.
531 48. Tschech A, Pfennig N. 1984. Growth-yield increase linked to caffeate reduction in
532 *Acetobacterium woodii*. Archives of Microbiology 137:163-167.
533 49. Hackmann TJ, Keyser BL, Firkins JL. 2013. Evaluation of methods to detect changes in
534 reserve carbohydrate for mixed rumen microbes. J Microbiol Methods 93:284-91.
535 50. Zhang B, Lingga C, Bowman C, Hackmann TJ. 2021. A new pathway for forming acetate
536 and synthesizing ATP during fermentation in bacteria. Appl Environ Microbiol
537 doi:10.1128/AEM.02959-20.
538 51. Hackmann TJ, Diese LE, Firkins JL. 2013. Quantifying the responses of mixed rumen
539 microbes to excess carbohydrate. Appl Environ Microbiol 79:3786-95.
540 52. Schönheit P, Wäscher C, Thauer RK. 1978. A rapid procedure for the purification of
541 ferredoxin from clostridia using polyethyleneimine. FEBS Lett 89:219-22.
542 53. Bradford MM. 1976. A rapid and sensitive method for the quantitation of microgram
543 quantities of protein utilizing the principle of protein-dye binding. Anal Biochem 72:248-
544 54.
545 54. Whitman WB (ed). 2022. Bergey's manual of systematics of archaea and bacteria. Wiley,
546 Oxford, United Kingdom.
547 55. Hackmann TJ, Zhang B. 2021. Using neural networks to mine text and predict metabolic
548 traits for thousands of microbes. PLoS Comput Biol 2:e1008757.
549 56. Chen IA, Chu K, Palaniappan K, Pillay M, Ratner A, Huang J, Huntemann M, Varghese
550 N, White JR, Seshadri R, Smirnova T, Kirton E, Jungbluth SP, Woyke T, Eloe-Fadrosh

EA, Ivanova NN, Kyrpides NC. 2019. IMG/M v.5.0: an integrated data management and comparative analysis system for microbial genomes and microbiomes. Nucleic Acids Res 47:D666-D677.

57. Kanehisa M, Furumichi M, Sato Y, Ishiguro-Watanabe M, Tanabe M. 2021. KEGG: integrating viruses and cellular organisms. Nucleic Acids Res 49:D545-D551.

58. Galperin MY, Makarova KS, Wolf YI, Koonin EV. 2015. Expanded microbial genome coverage and improved protein family annotation in the COG database. Nucleic Acids Res 43:D261-9.

59. Mistry J, Chuguransky S, Williams L, Qureshi M, Salazar GA, Sonnhammer ELL, Tosatto SCE, Paladin L, Raj S, Richardson LJ, Finn RD, Bateman A. 2021. Pfam: The protein families database in 2021. Nucleic Acids Res 49:D412-D419.

60. Sondergaard D, Pedersen CN, Greening C. 2016. HydDB: A web tool for hydrogenase classification and analysis. Sci Rep 6:34212.

61. Reimer LC, Vetcininova A, Carbasse JS, Sohngen C, Gleim D, Ebeling C, Overmann J. 2019. BacDive in 2019: bacterial phenotypic data for high-throughput biodiversity analysis. Nucleic Acids Res 47:D631-D636.

62. Mirdita M, Schütze K, Moriwaki Y, Heo L, Ovchinnikov S, Steinegger M. 2021. ColabFold-Making protein folding accessible to all. bioRxiv:doi: https://doi.org/10.1101/2021.08.15.456425.

63. Hackmann TJ. 2022. Redefining the coenzyme A transferase superfamily with a large set of manually annotated proteins. Protein Sci 31:864-881.

64. Zheng Y, Kahnt J, Kwon IH, Mackie RI, Thauer RK. 2014. Hydrogen formation and its regulation in *Ruminococcus albus*: involvement of an electron-bifurcating [FeFe]-

574 hydrogenase, of a non-electron-bifurcating [FeFe]-hydrogenase, and of a putative
575 hydrogen-sensing [FeFe]-hydrogenase. J Bacteriol 196:3840-52.
576 65. Zeikus JG, Fuchs G, Kenealy W, Thauer RK. 1977. Oxidoreductases involved in cell
577 carbon synthesis of *Methanobacterium thermoautotrophicum*. J Bacteriol 132:604-13.
578 66. Schoelmerich MC, Katsyv A, Donig J, Hackmann TJ, Muller V. 2020. Energy
579 conservation involving 2 respiratory circuits. Proc Natl Acad Sci USA 117:1167-1173.
580 67. Schönheit P, Wäscher C, Thauer RK. 1978. A rapid procedure for the purification of
581 ferredoxin from Clostridia using polyethyleneimine. FEBS letters 89:219-222.
582 68. Wang S, Huang H, Moll J, Thauer RK. 2010. $NADP^+$ reduction with reduced ferredoxin
583 and $NADP^+$ reduction with NADH are coupled via an electron-bifurcating enzyme
584 complex in *Clostridium kluyveri*. J Bacteriol 192:5115-23.
585 69. Heinonen JK, Lahti RJ. 1981. A new and convenient colorimetric determination of
586 inorganic orthophosphate and its application to the assay of inorganic pyrophosphatase.
587 Anal Biochem 113:313-7.

588

589 **TABLE 1.** Conditions used to measure enzymatic activity

Enzyme	Reference	Assay components[a,b]	Product measured (wavelength)	Controls	Conditions[c]
Glyceraldehyde-3-phosphate dehydrogenase (EC 1.2.1.12, 1.2.1.13, 1.2.1.59)	After Zheng et al. (64)	50 mM Tricine-Na (pH 8.4), 10 mM KPO_4 buffer (pH 7), 2 mM dithiothreitol (DTT), 2 mM $MgCl_2$, 1 mM glyceraldehyde 3-phosphate, 1 µg of cell extract protein, 1 mM NAD sodium salt or NADP disodium salt	Reduced NAD(P) (340 nm)[e]	Cell extract replaced with water	Aerobic
Malate dehydrogenase (EC 1.1.1.37, 1.1.1.82)	After Zeikus et al. (65)	50 mM Tris-Cl (pH 7.6), 0.2 mM NADH disodium salt or NADPH tetrasodium salt, 1 µg of cell extract protein, 2 mM oxaloacetic acid	Reduced NAD(P) (340 nm)[e]	Cell extract replaced with water	Aerobic
Pyruvate dehydrogenase (EC 1.2.4.1)	This study	50 mM Tris-Cl (pH 7.6), 10 mM $MgCl_2$, 4 mM DTT, 0.2 mM CoA lithium salt, 0.1 mM thiamine pyrophosphate, 4 U/mL phosphotransacetylase, 2 mM NAD sodium salt, 15.1 µg of cell extract or cytoplasmic contents protein, 10 mM sodium pyruvate	Reduced NAD (340 nm)[e]	Cell extract or cytoplasmic contents replaced with water	Anaerobic
Pyruvate:ferredoxin oxidoreductase (PFOR) (EC 1.2.7.1, 1.2.7.11)	After Zheng et al. (64)	50 mM Tris-Cl (pH 7.6), 10 mM $MgCl_2$, 4 mM DTT, 0.2 mM CoA lithium salt, 30 µM ferredoxin, 0.1 mM thiamine pyrophosphate, 4 U/mL phosphotransacetylase, 15.1 µg of cell extract or cytoplasmic contents protein, 10 mM sodium pyruvate	Reduced ferredoxin (430 nm)[f]	Cell extract or cytoplasmic contents replaced with water	Anaerobic
Rnf (Ferredoxin:NAD^+ oxidoreductase [Na^+-transporting]) (EC 7.2.1.2)	After Zheng et al. (64)	50 mM Tris-Cl (pH 7.6), 10 mM $MgCl_2$, 4 mM DTT, 10 mM NaCl, 80 µg of cell membrane protein (or 40 µg of solubilized cell membrane protein), reduced ferredoxin-regenerating system (0.2 mM	Reduced NAD (340 nm)[e]	Cell membrane replaced with water	Anaerobic

		CoA lithium salt, 30 µM ferredoxin, 0.1 mM thiamine pyrophosphate, 4 U/mL phosphotransacetylase, 36.2 µg of cytoplasmic contents protein, 10 mM sodium pyruvate), 2 mM NAD sodium salt			
Nqr (NADH:ubiquinone reductase [Na^+-transporting]) (EC 7.2.1.1)	This study	100 mM KPO_4 (pH 6), 100 mM NaCl, 4 mM DTT, 0.4 mM NADH disodium salt, 40 µg of solubilized cell membrane protein or 80 µg of cell membrane protein	Reduced NAD (340 nm)[e]	Cell membrane replaced with water	Anaerobic
Fumarate reductase/succinate dehydrogenase (EC 4.2.1.2)	After Asanuma and Hino (24)	100 mM KPO_4 (pH 6), 100 mM NaCl, 4 mM DTT, 0.4 mM NADH disodium salt, 40 µg of solubilized cell membrane protein or 80 µg of cell membrane protein, 5 mM disodium fumarate	Reduced NAD (340 nm)[e]	Fumarate and cell membrane replaced with water	Anaerobic
ATPase (EC 7.1.2.2)	After Schoelmerich et al. (66)	100 mM Tris-Cl (pH 7.4), 5 mM $MgCl_2$, 6.25 µg of cell membrane protein or solubilized cell membrane protein, 3.6 mM ATP-DiTris[d]	Phosphomolybdate (335 nm)[g]	None	Aerobic

[a]The components are listed in the order added (with the last component added to initiate the reaction)

[b]Source: NADH disodium salt, Sigma N8129; NADPH tetrasodium salt, Calbiochem 481973; oxaloacetic acid, Sigma O4126; coenzyme A lithium salt, Calbiochem 234101; ferredoxin, purified from *Clostridium pasteurianum* 5 according to Schönheit (67), phosphotransacetylase, Megazyme E-PTABS; crude pyruvate:ferredoxin oxidoreductase, cytoplasmic contents from same bacterium being assayed for activity

595 [c]Anaerobic conditions were 1 mL assay mix in 1.4 mL glass cuvette (Hellma HL114-10-20) capped with chlorobutyl stopper (DWK
596 Life Sciences W224100-081) under N_2 at 37°C; aerobic conditions were 0.2 mL assay mix in 96-well plates at room temperature;
597 aerobic conditions for ATPase assay were 0.1 mL assay mix in 1.5 mL tube at 37°C
598 [d]Mix was incubated for 0, 4, 8, and 12 min and reaction terminated by adding 14.3 µL of 30% (w/v) trichloroacetic acid
599 [e]Extinction coefficient of 6,200 M^{-1} cm^{-1} (64)
600 [f]Extinction coefficient of 13,100 M^{-1} cm^{-1} (68)
601 [g]Phosphomolybdate was formed by adding 90 µL supernatant with 450 µL of AAM-reagent (69) and incubating for 10 min at room
602 temperature; phosphate was the standard
603

TABLE 2. Enzymatic assays confirm *Prevotella* catalyze key reactions for forming propionate, succinate, and acetate

Reaction ID[a]	Reaction equation	Source	*P. brevis* GA33		*P. ruminicola* 23	
			Activity[b,c]	*P*-value	Activity[b,c]	*P*-value
6	D-Glyceraldehyde-3-phosphate + Orthophosphate + NAD^+ <=> 3-Phospho-D-glyceroyl phosphate + NADH + H^+	Cell extract	2814 (190)	<0.001	2840 (360)	0.008
11	2 Reduced ferredoxin + Acetyl-CoA + CO_2 + 2 H^+ <=> 2 Oxidized ferredoxin + Pyruvate + CoA	Cell extract	346 (97)	0.035	449 (92)	0.020
		Cytoplasmic contents	290 (20)	0.002	291 (84)	0.037
15	(S)-Malate + NAD^+ <=> Oxaloacetate + NADH + H^+	Cell extract	979 (30)	<0.001	2420 (260)	0.006
22	NADH + H^+ + ubiquinone + n Na^+[side 1] = NAD^+ + ubiquinol + n Na^+[side 2]	Membrane	17.8 (5.6)	0.043	16.4 (2.6)	0.012
		Solubilized membrane	28.8 (1.7)	0.002	17.2 (3.8)	0.022
23	Quinone + Succinate <=> Hydroquinone + Fumarate	Membrane	155.3 (8.9)	0.002	27.5 (5.4)	0.018
		Solubilized membrane	420 (33)	0.003	42.2 (5.9)	0.009
24	ATP + H_2O + 4 H^+[side 1] = ADP + phosphate + 4 H^+[side 2]	Membrane	97 (23)	0.025	53.3 (1.7)	0.001
		Solubilized membrane	102 (16)	0.012	61.5 (4.2)	0.002
25	D-Glyceraldehyde-3-phosphate + Orthophosphate + $NADP^+$ <=> 3-Phospho-D-glyceroyl phosphate + NADPH + H^+	Cell extract	515 (24)	<0.001	214 (120)	0.106
26	(S)-Malate + $NADP^+$ <=> Oxaloacetate + NADPH + H^+	Cell extract	501.5 (6.7)	<0.001	216 (25)	0.007

[a]See Fig. 5, Table S3, and Table S4 for more information

[b]Units are mean (SEM) mU/(mg protein)

607 [c]Results are for at least of 3 biological replicates (cell extract or membrane prepared from independent cultures)

608 **Figure legends**

609 **Fig. 1.** Fermentation of glucose to propionate, succinate, and acetate has missing or unknown steps**.**
610 (A) The missing steps are for regenerating redox cofactors. (B) We hypothesize Rnf carries out
611 the missing steps. Abbreviations: Fd_{ox}, oxidized ferredoxin; Fd_{red}, reduced ferredoxin (two reduced
612 iron-sulfur clusters); NAD_{ox}, oxidized NAD; NAD_{red}, reduced NAD.

613

614 **Fig. 2.** *Prevotella* form propionate, succinate, and acetate during fermentation of glucose. (A)
615 Yield of fermentation products. (B) Recovery of carbon is near or above 100%. (C) Recovery of
616 hydrogen is also near or above 100%. (D) Summary of growth and fermentation. In (A), the yield
617 of cells is g $(mmol\ glucose)^{-1}$. Results are mean ± standard error of at least 3 biological replicates
618 (culture supernatant or cells prepared from independent cultures).

619

620 **Fig. 3.** *Prevotella* have the enzyme Rnf. Rnf is evident in the (A) genome, (B) proteome, and (C)
621 measurements of enzyme activity. Results in (C) are mean ± standard error of 3 biological
622 replicates (cell membranes prepared from independent cultures). To correct Rnf for activity of
623 NADH dehydrogenase, we added the activity measured for Nqr (see Table 2). Abbreviations:
624 Fd_{ox}, oxidized ferredoxin; Fd_{red}, reduced ferredoxin (two reduced iron-sulfur clusters); NAD_{ox},
625 oxidized NAD; NAD_{red}, reduced NAD; DDA, data-dependent acquisition; DIA, data-independent
626 acquisition; Membrane, cell membrane sample; Solb membr, solubilized cell membrane sample.
627 See Tables S3 and S4 for more information.

628

Fig. 4. *Prevotella brevis* GA33 depends on Na^+ for growth and for Rnf activity. In (A), sodium was removed from the media by replacing NaCl, NaOH and Na_2CO_3 with equimolar KCl, KOH, and K_2CO_3. Resazurin was also removed. Results are for one representative culture. Experiments were done with 2 cultures on 2 different days. In (B), sodium was removed from the assay mix by replacing NAD sodium salt, sodium pyruvate, and CoA lithium salt with equimolar NAD hydrate, potassium pyruvate, and CoA hydrate. The residual Na^+ in the Tris-Cl buffer and $MgCl_2$ was 2 μM (as measured by an electrode; Fisher Accumet 13-620-503A). No correction was made for NADH dehydrogenase activity. Results are mean ± standard error of 4 biological replicates (cell membranes prepared from independent cultures).

Fig. 5. *Prevotella* have enzymes for forming propionate, succinate, and acetate in the proteome. (A) Cytoplasmic enzymes. (B) Rnf and other membrane-bound enzymes. Abbreviations: Glc-6P, glucose-6-phosphate; Fru-6P, fructose-6-phosphate; F1,6BP, fructose-1,6-bisphophate; G3P, glyceraldehyde-3-phosphate; DHAP, dihydroxyacetone phosphate; 1,3BGP, 1,3-bisphosphoglycerate; 3PG, 3-phosphoglycerate; 2PG, 2-phosphoglycerate; PEP, phosphoenolpyruvate; Pyr, pyruvate; Ac-CoA, acetyl-CoA; Ac-P, acetyl-phosphate; OAA, oxaloacetate; Mal, malate; Fum, fumarate; Suc-CoA, succinyl-CoA; L-MM-CoA, L-methylmalonyl-CoA; D-MM-CoA, D-methylmalonyl-CoA; Pr-CoA, propionyl-CoA; Fd_{ox}, oxidized ferredoxin; Fd_{red}, reduced ferredoxin (two reduced iron-sulfur clusters); NAD_{ox}, oxidized NAD; NAD_{red}, reduced NAD; CoA, coenzyme A; P_i, inorganic phosphate; Q_{ox}, oxidized quinone; Q_{red}, reduced quinone. See Tables S3 and S4 for more information.

651 **Fig. 6.** Many organisms form propionate, succinate, and acetate during fermentation. Organisms
652 (n = 1,436) and their reported end products (n = 39) are from *Bergey's Manual of Systematics of*
653 *Archaea and Bacteria* (54). Minor (trace) end products are not included. Abbreviations: Ac,
654 acetate; Suc, succinate; Pr, propionate. See Table S5 for more information.

655

656 **Fig. 7.** Rnf may be used by many prokaryotes that form propionate, succinate, and acetate during
657 fermentation. (A) Alluvial graph showing percentage of prokaryotes with Rnf genes. Rnf genes
658 are enriched in organisms that are fermentative and form propionate, succinate, and acetate. (B)
659 Phylogenetic tree of prokaryotes, highlighting those with Rnf genes and that form propionate,
660 succinate, and acetate during fermentation. (C) Habitats of prokaryotes with Rnf genes and
661 observed to form propionate, succinate, and acetate during fermentation. Abbreviations: Ac,
662 acetate; Suc, succinate; Pr, propionate. See Tables S5, S6, and S7 for more information.

663

Figure 1

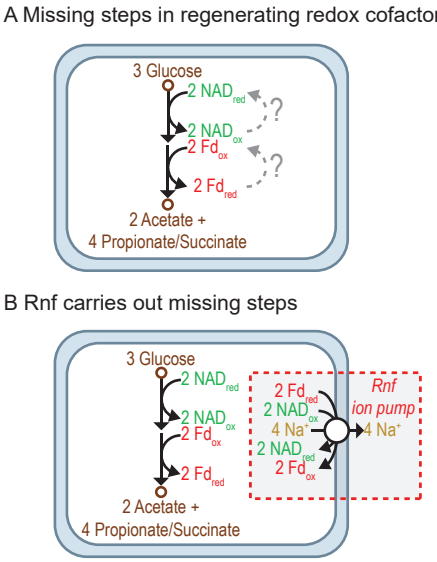

Figure 2

Prevotella brevis GA33

Prevotella ruminicola 23

A Fermentation products

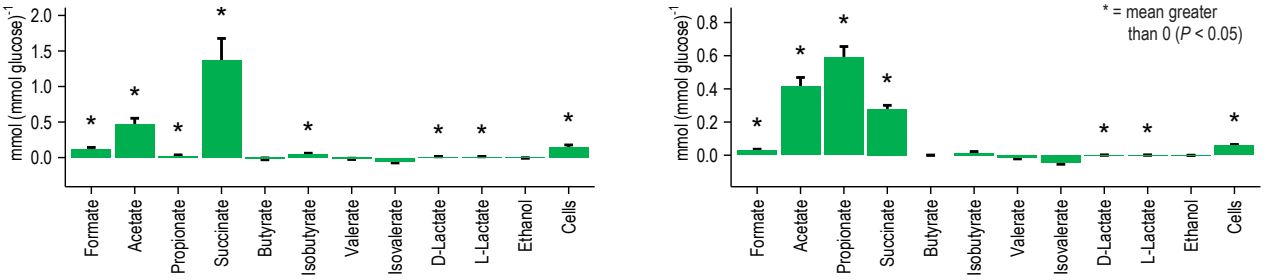

B Carbon recovery

Time	Glucose	Acids	CO_2	Cells	Total
	mean (SEM) mmol C L^{-1}				
Start	93.3 (8.7)	103.3 (0.8)	0 (0)	0 (0)	196.6 (8.3)
End	58.8 (2.6)	136.7 (4.2)	-5.1 (0.6)	31.3 (1.3)	221.7 (4.8)
				Recovery	**113.2 (4.3) %**

Time	Glucose	Acids	CO_2	Cells	Total
	mean (SEM) mmol C L^{-1}				
Start	232 (14)	57.0 (2.0)	0 (0)	0 (0)	289 (15)
End	78.1 (2.1)	144.6 (4.4)	1.6 (1.5)	61.1 (0.3)	285.0 (5.0)
				Recovery	**99.3 (6.7) %**

C Hydrogen recovery

Time	Glucose	Acids	H_2O	Cells	Total
	mean (SEM) mmol H L^{-1}				
Start	187 (17)	206.6 (1.6)	0 (0)	0 (0)	393 (17)
End	117.5 (5.1)	259.0 (7.0)	9.3 (1.2)	55.0 (1.9)	441.0 (9.5)
				Recovery	**112.6 (4.3) %**

Time	Glucose	Acids	H_2O	Cells	Total
	mean (SEM) mmol H L^{-1}				
Start	465 (28)	114.0 (4.0)	0 (0)	0 (0)	579 (30)
End	156.3 (4.2)	275.0 (8.7)	23.0 (0.1)	112.7 (2.3)	566.9 (5.3)
				Recovery	**98.5 (5.8) %**

D Summary

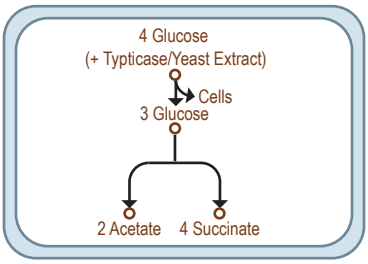

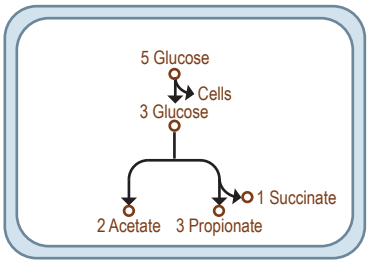

Figure 3

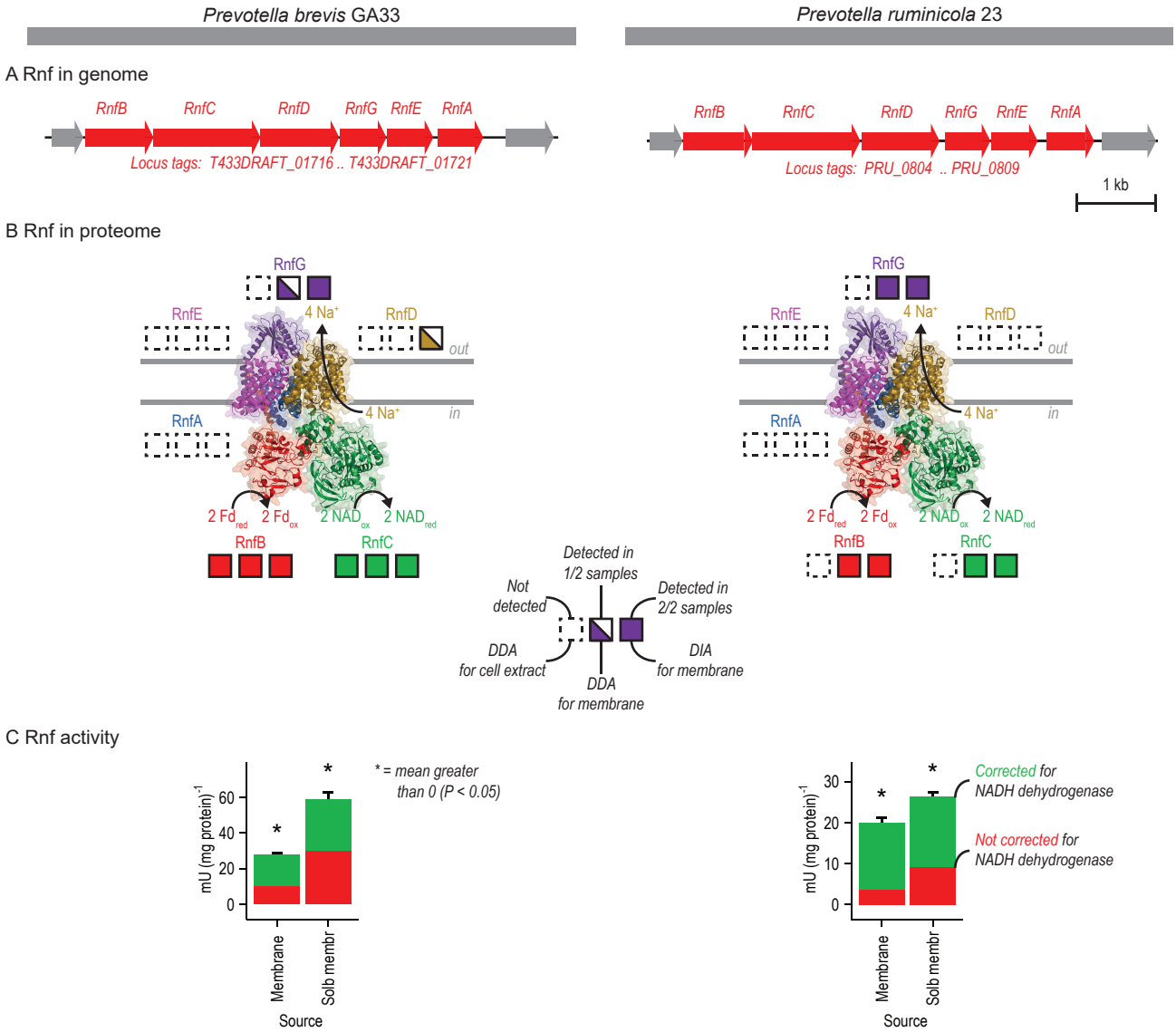

Figure 4

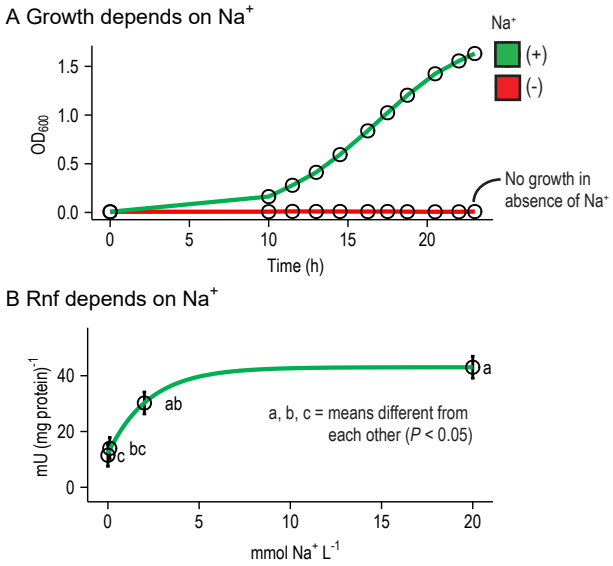

Figure 5

Prevotella brevis GA33 *Prevotella ruminicola* 23

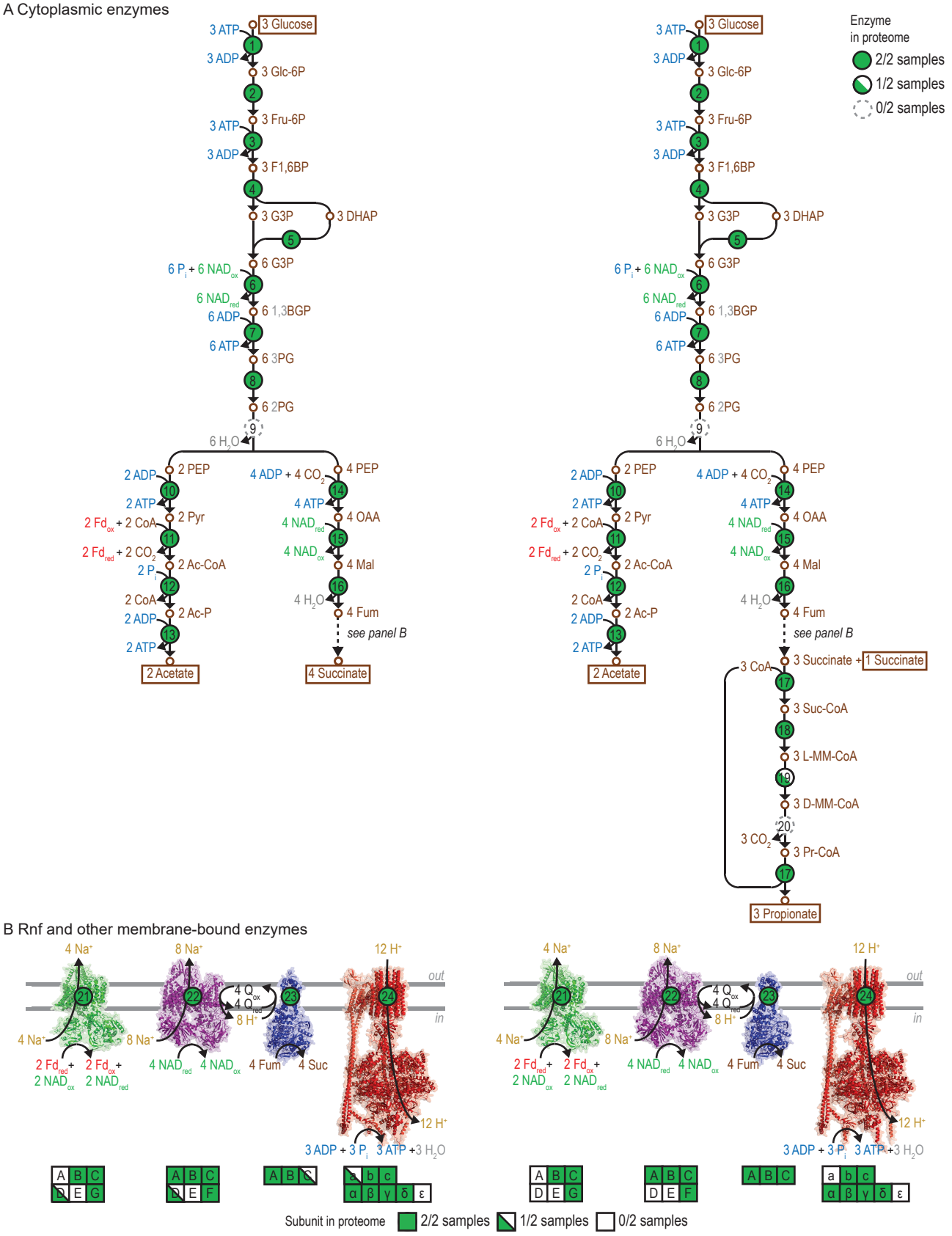

Figure 6

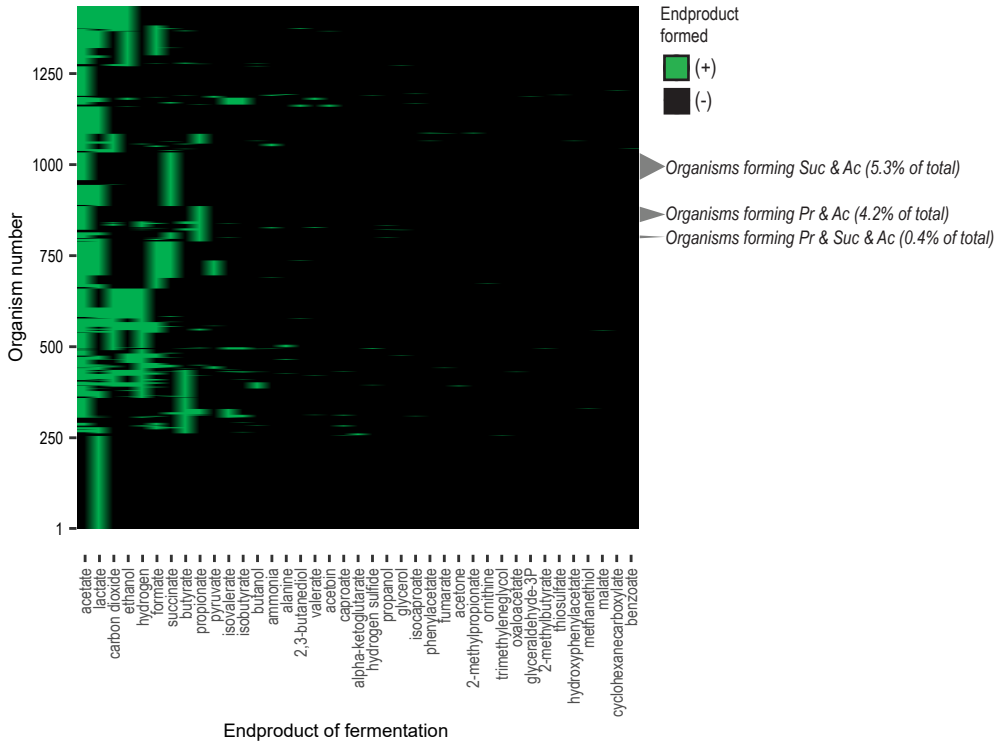

Figure 7

A Alluvial graph

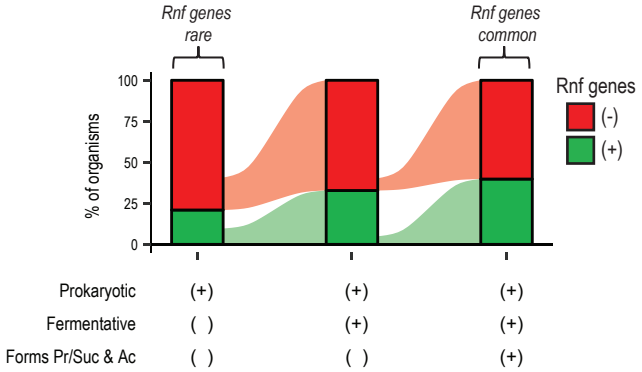

B Phylogenetic tree

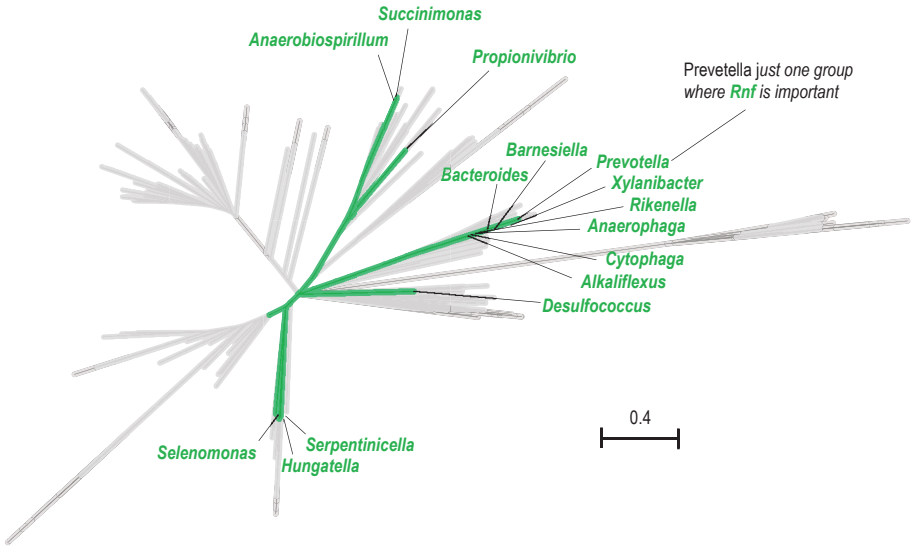

C Habitats